Dependence of multiple-scattering distributions on the charge states of fast ions exiting from solid targets

E. P. Kanter
Physics Division, Argonne National Laboratory, Argonne, Illinois 60439
(Received 4 March 1983)

Measurements are reported on the multiple-scattering widths for 1–4-MeV N^+ projectiles in thin carbon targets as a function of the charge state of the outgoing ion. Evidence is found for a significant enhancement of the angular widths for K-vacancy–bearing emergent ions. A quantitative model is proposed demonstrating how the "memory" of K-vacancy–producing collisions can give rise to such an enhancement despite apparent charge-state equilibration.

I. INTRODUCTION

In studies concerned with energetic heavy-ion beams in solids, it is generally assumed that for target thicknessses larger than those required to achieve "charge-state equilibrium," the multiple-scattering widths of emergent-ion angular distributions are independent of the final charge state. The equilibrium length is usually defined as the minimum target thickness for which the final charge-state distributions remain constant when foil thickness and/or incident beam charge state are varied.[1] In practice, the mean charge state of the emerging ions or the distribution of charge states near the mean charge is used as a quantitative test of this constancy.[2]

The multiple scattering experienced by swift heavy ions traversing matter has received much attention by theorists and experimentalists alike (see, for example, Refs. 3–8, and references contained therein). It has become common practice to compare multiple-scattering distributions measured for projectiles (regardless of their charge state) emerging from thin foils or gaseous targets with predictions based on the theory of Meyer[3] (or the more recent treatment of Sigmund and Winterbon[4]) and agreement is generally excellent (e.g., Refs. 7 and 8). These theories assume charge-exchange equilibration in the foil and use screened ion-atom potentials characterized by a *constant* mean charge. This therefore results in multiple-scattering distributions that are independent of the final charge state.

Measurements of the angular distributions of ultrahigh–charge-state (charge states far above the mean) ions produced by stripping of heavy-ion beams in dilute gas targets have demonstrated that these rare charge states are produced primarily by single violent collisions.[9] We have measured the angular distributions of ultrahigh–charge-state ions emerging from solid targets and find that for target thicknesses well in excess of the "normal equilibrium" length, such ions retain the "memory" of a single small–impact-parameter collision. We show that this effect leads to a marked charge-state dependence of measured angular distributions which must be considered in experimental tests of multiple-scattering theories. Furthermore, we demonstrate that such angular-distribution measurements can yield important information about the individual scattering events experienced by fast ions penetrating condensed matter.

II. EXPERIMENT

The apparatus is essentially that used in recent measurements[10] on the dissociation of molecular-ion beams produced by Argonne's 4.5-MeV Dynamitron accelerator. Magnetically analyzed ion beams were collimated to have a maximum angular divergence of ± 0.09 mrad at the target position. Sets (both horizontal and vertical) of "predeflector" and "postdeflector" plates permitted electrostatic deflection of the beam incident upon and emerging from the target foil. A 25° electrostatic analyzer (ESA) having a relative energy resolution of 6×10^{-4} [full width at half maximum (FWHM)], and offset by 2 mrad horizontally from the direction of the undeflected incident beam, was located several meters downstream from the target. A silicon surface-barrier detector counted particles emerging from the exit slit of the analyzer. Distributions in energy and angle were determined for particles emerging from the target by varying the voltages on the horizontal predeflectors and/or the postdeflectors in conjunction with that on the ESA. The overall angular resolution was 0.3 mrad (FWHM). Target thicknesses were measured by energy-loss techniques with an accuracy of $\pm 10\%$.

The complete joint energy-angle distributions will be the subject of a planned future publication. The measurements described in this paper consist of scans of the horizontal postdeflector voltages with the ESA set to analyze the most probable final energy for each emergent charge state. Additional measurements were performed with a fixed voltage on the postdeflector plates and with a movable silicon surface-barrier detector collimated to 0.19 mrad. With this latter technique energy-integrated angular distributions were obtained. These distributions were consistent with those taken with the ESA.

III. RESULTS

Two charge-state distributions obtained (at 0°) from the movable detector measurements are shown in Fig. 1. These distributions are in accord with measurements for

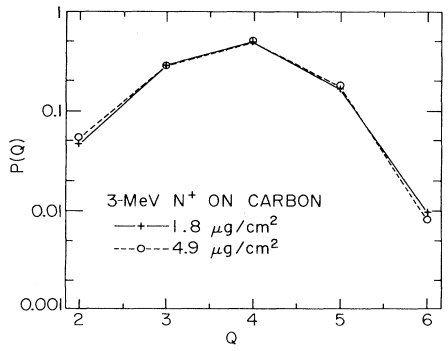

FIG. 1. Energy- and angle-integrated distributions of final charge states of nitrogen ions exiting near 0° from 1.8- and 4.9-$\mu g/cm^2$ carbon foils bombarded by a 3-MeV N^+ beam.

6- and 16-$\mu g/cm^2$ targets.[11,12] Comparisons of the means (3.80 and 3.81), standard deviations (0.79 and 0.81), and skewnesses (−0.067 and −0.135) of these distributions measured with 1.8- and 4.9-$\mu g/cm^2$ carbon targets, respectively, would lead to the assumption that charge-state equilibration had already been achieved in the thinner target.

In contrast with the charge-state distributions, the angular distributions for each charge state display characteristic nonequilibrium behavior. Figure 2 shows angular distributions for the eight charge states of nitrogen (N^{+q}, $q=0-7$) that were observed after passage of a 3.7-MeV N^+ beam through a 1.6-$\mu g/cm^2$ carbon target. The distributions for $q=0-5$ are qualitatively similar (though quantitative comparisons reveal distinct trends with charge state). The widths are in agreement with theoretical estimates.[3] The distributions for N^{+6} and N^{+7} are, however, distinctly different from those for the lower charge states. A significant increase in the widths of these distributions is readily apparent. Also evident is a slight "dip" at 0° in the N^{+7} distribution. The N^{+6} and N^{+7} ions contain K vacancies upon exiting from the target and have, with high probability, experienced one or more violent small—impact-parameter collisions in the foil. Such collisions are not very frequent and so do not significantly affect the angular distributions for the lower charge states.

These data are representative of more extensive measurements utilizing 1—4 MeV beams of C^+, O^+, N^+, and Ne^+ in targets of carbon and aluminum ranging in thicknesses from 1—20 $\mu g/cm^2$. The results may be summarized as follows.

(1) For each combination of beam, energy, and target, there is a marked increase in the widths of the angular distributions of the two (and sometimes three) highest exiting charge states observed, even for the thickest targets used.

(2) The increase in width is most dramatic for the lowest energies and thinnest targets employed.

(3) The second moments of these angular distributions are a monotonically increasing function of charge state.

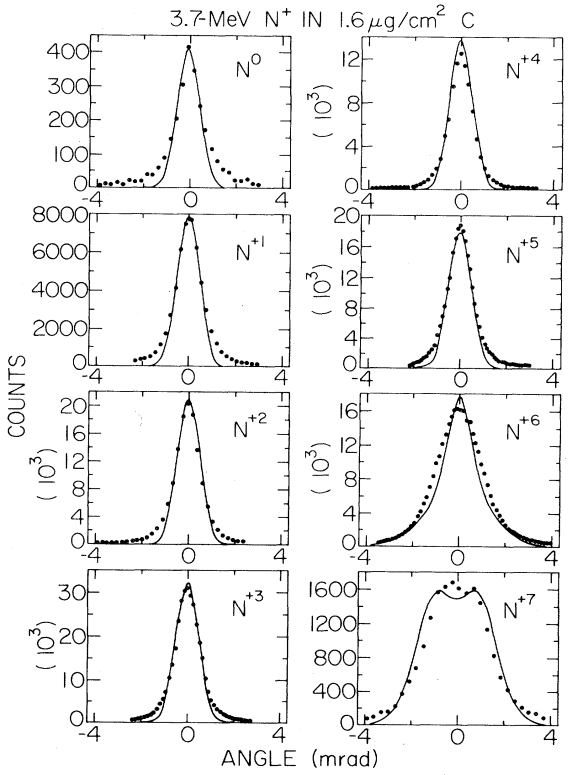

FIG. 2. Angular distributions, measured with the ESA as described in the text, of nitrogen particles in all final charge states emerging from a 1.6-$\mu g/cm^2$ carbon target after impact of 3.7-MeV N^+ ions. Solid lines are calculated angular distributions, using the model described in text, corresponding to the experimental conditions of the data (filled points).

IV. DISCUSSION

We have been able to reproduce these features of the data quantitatively with a simple two-component model for the passage of the ions through the solid. Such models have been successful in explaining the development of projectile K vacancies in experiments with energetic heavy-ion beams traversing solids.[13—15] In our model, we divide the target into 5-Å-thick layers and consider the histories of two beam components during the target dwell time—those ions with either one or no electrons in the K shell and those with filled K shells. Small—impact-parameter scattering events leading to the creation of K-shell vacancies are assumed to redistribute the resulting projectile ions into an angular distribution with a hollow center, similar to those observed in single-collision experiments with gaseous targets[16,17] and with solid targets of nonequilibrium thicknesses.[18] The net effect of all other collisions in the target is assumed (for simplicity) to smear the distributions of both beam components with a Gaussian profile in each 5-Å layer of the target. The width of this Gaussian is chosen to give the measured "normal" multiple-scattering width for the component with a filled K shell after traversal of the entire target thickness. The final yields of the two components are determined, as are

the exchange probabilities in each layer, by the cross sections for vacancy production and destruction.

The angular distributions for the two components are computed by numerical integrations for the required target thickness. The details of that calculation are described in the Appendix. The two distributions are then combined, with appropriate weights, to produce angular distributions for each final charge state. The weighting factors are chosen to yield the correct final distribution of charge states. The distributions of these weighting factors with respect to charge state are assumed to be Gaussians of equal width for the two components with the mean charge of the vacancy-bearing component shifted upwards by two charge states to account for both the presence of the K vacancies and further Auger deexcitation outside the target. Because of these constraints, the only adjustable parameters in the calculation are the two cross sections and the width parameter for the hollow-center single-scattering distribution. The cross sections determined in this way were typically in the range $10^{-19}-10^{-17}$ cm^2. As an example, for 3.7-MeV N^+ in carbon, we find K-vacancy production and destruction cross sections of 0.2×10^{-18} and 6.3×10^{-18} cm^2, respectively. There are no reliable previous measurements of such cross sections for carbon targets. However, there is an abundance of related data available from studies of single-collision charge-changing processes in gaseous targets.[1] For comparison Nikolaev *et al.*[19] report that for 4.6-MeV N^+ in dilute N_2 gas, $\sigma(N^{+5}\rightarrow N^{+6})\simeq3\times10^{-18}$ cm^2.

The results of a typical calculation with this model are shown in Fig. 2. Figure 3 shows a comparison of the fitted widths from these distributions with the experimental results derived from angular distributions such as those in Fig. 2. More detailed comparisons than these do not seem appropriate at present because of the underlying limitations of this computationally simple model. The long, non-Gaussian tails evident in the data (Fig. 2) strongly influence the second and higher moments of the distributions and cannot be reproduced within the framework of this model. The calculation does, however, produce angular distributions whose second moments increase with charge state, as the presence of the vacancy-bearing component becomes important. The calculation also reproduces the 0° "dips" seen in the angular distributions of the highest charge states.

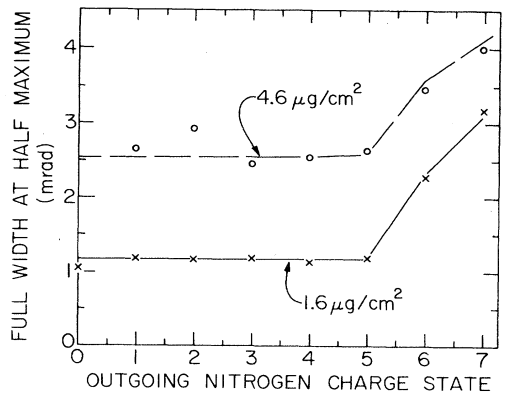

FIG. 3. Full width at half maximum (FWHM) of angular distributions of nitrogen ions emerging in various charge states from 1.6- and 4.6-μg/cm^2 carbon targets following impact of 3.7-MeV N^+ ions. Points are the FWHM's of best-fit Gaussian profiles to the data. Lines result from similar analyses of the angular distributions derived for each charge state from the model described in the text using the same parameters for both target thicknesses.

V. CONCLUSIONS

These results demonstrate that despite the apparent equilibration of the central charge-state distributions, it is possible to observe remnant behavior characteristic of *single-scattering events* when energetic heavy-ion beams traverse thin solid targets. It is important to recognize the presence of such effects in any experimental tests of heavy-ion multiple-scattering theories. Furthermore, this phenomenon should be considered in the design of heavy-ion stripping systems where the desire for large yields of the high charge states must be balanced against the increased multiple-scattering widths reported here. Recent confirmation[20] of the nonequilibration of K-shell charge-exchange processes in this thickness regime has also been found in measurements of the yield of KLL Auger electrons from 3-MeV N^+ beams exiting solid carbon targets. It is hoped that further refinements to the model described here will yield accurate electron capture and loss cross sections as well as details of the single-scattering angular distributions in the solid medium.

ACKNOWLEDGMENTS

The author would like to thank D. S. Gemmell, I. Plesser, and W. J. Pietsch for their efforts during various phases of the experiments described here. This work was supported by the U.S. Department of Energy, Office of Basic Energy Sciences, under Contract No. W-31-109-Eng-38.

APPENDIX

We divide the ion beam into two components. The fraction containing a K vacancy is designated f_1 while the remaining non-vacancy-bearing fraction is f_0. The double vacancy fraction is presumed to be negligible. Assuming cross sections σ_c and σ_l for K-electron capture and loss, respectively, it is easy to show that if $f_1(0)=0$, the vacancy-bearing fraction of the beam will develop with target depth z as

$$f_1(z)=\frac{\sigma_l}{\sigma}(1-e^{-n\sigma z}) , \tag{A1}$$

where $\sigma=\sigma_l+\sigma_c$. The angular distributions of these two components will display a similar approach to equilibrium.

Consider the fractional velocity densities $Q_i(u,\phi,z)$ $(i=0,1)$, where u and ϕ are the cylindrical coordinates of transverse velocity space of the beam such that

$$f_i=\int_0^{2\pi}\int_0^{\infty}Q_i(u,\phi,z)u\,du\,d\phi . \tag{A2}$$

For each slice Δz, there is a probability p_l for each of the f_0 nonvacancy particles (independent of u,ϕ) to undergo K-shell ionization. Likewise the probability p_c describes the filling of vacancies in the f_1 population. The angular distributions to describe these charge-changing collision processes are cylindrically symmetric and denoted by properly normalized functions $g_l(|\Delta\vec{u}|)$ and $g_c(|\Delta\vec{u}|)$ where $\Delta\vec{u}$ is the change in transverse velocity resulting from these collisions. Similarly the function $g(|\Delta\vec{u}|)$ is used to smear the non-charge-changing fractions.

Because of the cylindrical symmetry, we drop the angle ϕ and write for the changes in Q_i in the slice Δz

$$\Delta Q_0(u,z)=\int_0^{2\pi}\int_0^{\infty}[Q_0(R,z)(1-p_l)g(u')+Q_1(R,z)p_c g_c(u')]u'du'd\theta'-Q_0(u,z)p_l\ , \tag{A3a}$$

$$\Delta Q_1(u,z)=\int_0^{2\pi}\int_0^{\infty}[Q_1(R,z)(1-p_c)g(u')+Q_0(R,z)p_l g_l(u')]u'du'd\theta'-Q_1(u,z)p_c\ , \tag{A3b}$$

$$R^2=u^2+u'^2+2uu'\cos\theta'\ . \tag{A3c}$$

By proper choice of the functions $g_i(u)$, these integrals can be made tractable. We choose the forms

$$g_l(u)=\frac{n}{\pi U_l^4}u^2\exp\left[\frac{-nu^2}{U_l^2}\right] \tag{A4a}$$

and

$$g(u)=g_c(u)=\frac{n}{\pi U^2}\exp\left[\frac{-nu^2}{U^2}\right]\ , \tag{A4b}$$

where n is the number of $\Delta z=5$ Å steps in the target and U is the product of the "normal" multiple-scattering root-mean-square angle and the ion beam velocity.

By combining Eqs. (A3) and (A4) and substituting for u'^2, the resulting pair of equations can be cast into a form which can be conveniently integrated using a Gauss-Laguerre quadrature formula. The functions Q_0 and Q_1 are sufficiently smooth that a ten-point quadrature was found to be adequate to carry out the u' integrations. The θ' integrals are done by trapezoidal rule.

[1]H. D. Betz, Rev. Mod. Phys. 44, 465 (1972).
[2]W. N. Lennard, T. E. Jackman, and D. Phillips, Phys. Lett. 79A, 309 (1980).
[3]L. Meyer, Phys. Status Solidi B 44, 253 (1971).
[4]P. Sigmund and K. B. Winterbon, Nucl. Instrum. Methods 119, 541 (1974).
[5]D. A. Eastham, Nucl. Instrum. Methods 125, 277 (1975).
[6]W. Möller, G. Pospiech, and G. Schrieder, Nucl. Instrum. Methods 130, 265 (1975).
[7]H. H. Andersen, J. Bøttiger, H. Knudsen, P. Møller Petersen, and T. Wohlenberg, Phys. Rev. A 10, 1568 (1974).
[8]G. Spahn and K.-O. Groeneveld, Nucl. Instrum. Methods 123, 425 (1975).
[9]G. Ryding, A. Wittkower, and P. H. Rose, Phys. Rev. A 3, 1658 (1971).
[10]B. J. Zabransky, P. J. Cooney, D. S. Gemmell, E. P. Kanter, and Z. Vager, Rev. Sci. Instrum. 54, 531 (1983).
[11]R. Girardeau, E. J. Knystautas, G. Beauchemin, B. Neveu, and R. Drouin, J. Phys. B 4, 1743 (1971).
[12]E. J. Knystautas and M. Jomphe, Phys. Rev. A 23, 679 (1981).
[13]T. J. Gray, C. L. Cocke, and R. K. Gardner, Phys. Rev. A 16, 1907 (1977).
[14]C. L. Cocke, S. L. Varghese, and B. Carnutte, Phys. Rev. A 15, 874 (1977).
[15]F. Hopkins, J. Sokolov, and A. Little, Phys. Rev. A 15, 588 (1977).
[16]B. Efken, D. Hahn, D. Hilscher, and G. Wüstefeld, Nucl. Instrum. Methods 129, 227 (1975).
[17]C. D. Moak, IEEE Trans. Nucl. Sci. NS-23, 1126 (1976).
[18]G. D. Alton, J. A. Biggerstaff, L. Bridwell, C. M. Jones, Q. Kessel, P. D. Miller, C. D. Moak, and B. Wehring, IEEE Trans. Nucl. Sci. NS-22, 1685 (1975).
[19]V. S. Nikolaev, I. S. Dmitriev, Yu. A. Tashaev, Ya. A. Teplova, and Yu. A. Fainberg, J. Phys. B 8, L58 (1975).
[20]D. Schneider, E. P. Kanter, and B. J. Zabransky, Phys. Rev. A 26, 3700 (1982).